6-1-2018

A High-Throughput Screening Assay for Pyruvate Carboxylase

Brittney N. Wyatt
Marquette University

Leggy A. Arnold
University of Wisconsin - Milwaukee

Martin St. Maurice
Marquette University, martin.stmaurice@marquette.edu

Accepted version. *Analytical Biochemistry*, Vol. 550 (June 1, 2018): 90-98. DOI.

Analytical Biochemistry, Vol. 550, (June 1, 2018): 90-98. DOI.

A High-Throughput Screening Assay for Pyruvate Carboxylase

Brittney N. Wyatt
Department of Biological Sciences, Marquette University, Milwaukee, WI
Leggy A. Arnold
Department of Chemistry and Biochemistry and Milwaukee Institute for Drug Discovery, University of Wisconsin-Milwaukee, Milwaukee, WI
Martin St. Maurice
Department of Biological Sciences, Marquette University, Milwaukee, WI

Abstract

Pyruvate carboxylase (PC) catalyzes the conversion of pyruvate to oxaloacetate (OAA), an important metabolic reaction in a wide range of organisms. Small molecules directed against PC would enable detailed studies on the metabolic role of this enzyme and would have the potential to be developed into pharmacological agents. Currently, *specific* and *potent* small molecule regulators of PC are unavailable. To assist in efforts to find, develop, and

characterize small molecule effectors of PC, a novel fixed-time assay has been developed based on the reaction of OAA with the diazonium salt, Fast Violet B (FVB), which produces a colored adduct with an absorbance maximum at 530 nm. This fixed time assay is reproducible, sensitive and responsive to known effectors of *Rhizobium etli* PC, *Staphylococcus aureus* PC, and *Listeria monocytogenes* PC, and is highly amenable to high-throughput screening. The assay was validated using a plate uniformity assessment test and a pilot screen of a library of 1280 compounds. The results indicate that the assay is suitable for screening small molecule libraries to find novel small molecule effectors of PC.

Keywords

Pyruvate carboxylase, Diazonium salt, Fast violet B, Oxaloacetate, High throughput screening

Introduction

Pyruvate carboxylase (PC) is a biotin-dependent metabolic enzyme that catalyzes the conversion of pyruvate to oxaloacetate (OAA) through a MgATP-dependent carboxyl group transfer from HCO_3^- to pyruvate. The reaction occurs in two distinct active sites located in the biotin carboxylase (BC) and the carboxyltransferase (CT) domains of the enzyme [1]. A tethered biotin cofactor is initially carboxylated by HCO_3^- in the BC domain, with the concomitant cleavage of MgATP. The carboxybiotin cofactor is subsequently transferred to the CT domain, which facilitates the carboxyl group transfer from carboxybiotin to pyruvate, forming OAA [1]. This anaplerotic reaction serves to replenish tricarboxylic acid cycle (TCA) intermediates that are lost to alternative biosynthetic reactions [2]. Recent studies have linked aberrant PC activity to several diseases and infections, such as type 2 diabetes, listeriosis, and certain types of cancers [3, 4, 5, 6, 7, 8, 9, 10]. Many of these studies have revealed a correlation between reduced PC expression/activity and decreased insulin release, while enhanced PC expression and activity has been associated with tumor cell proliferation and breast cancer metastases [3,4,7,11]. Additionally, PC is necessary for the pathogenicity of *Listeria monocytogenes*, a facultative intracellular bacterium [8,12,13].

While there is a growing realization that PC activity is implicated in a wide range of diseases and infections, at present, there are no *specific* and *potent* small molecule effectors available to study altered PC activity *in vitro* or *in vivo*. A number of small molecules are known to alter PC activity [14,15], but none of these demonstrate high binding affinities and many of them are promiscuous. Oxalate for example, is an inhibitor of PC with a K_i value of 12 μM (chicken liver PC [14]), but is also a known metal chelator [16] that inhibits lactate dehydrogenase (LDH) [17] and transcarboxylase [18]. Specific and potent small molecule effectors have great potential to be used as biochemical tools to aid in delineating the structure, mechanism, and regulation of PC, as well as informing on its role in infection and disease. The development of a high-throughput assay is an important prerequisite in discovering new and potent effectors of PC activity.

Several well-established coupled-enzyme assays are available to study PC activity [19,20], but none of these are well suited to high throughput screening (HTS) of small molecule effectors. The PC-catalyzed carboxylation of pyruvate is typically measured by coupling the formation of

the product, OAA, to the malate dehydrogenase (MDH) catalyzed reduction of OAA to malate and oxidation of NADH to NAD^+ [20]. In addition, there are a variety of other coupled-enzyme assays that can measure the specific half-reactions catalyzed in either the BC or CT domains. For example, an LDH-coupled assay can be used to determine the rate of OAA decarboxylation in the CT domain by the NADH-dependent reduction of pyruvate to lactate. Similarly, a glucose-6-phospate dehydrogenase/phosphoglucomutase/phosphorylase coupled assay system can be used to determine the rate of MgATP cleavage in the BC domain [19]. These coupled-enzyme assays are generally inappropriate for screening large libraries of small molecules. For instance, the inclusion of secondary coupling enzymes raises the potential for small molecules to target the coupling enzyme instead of, or in addition to, the target enzyme. While counter-screens of small molecules against the coupling enzyme are routinely implemented in HTS programs, these represent an additional step that must be performed to eliminate false positives [21,22]. Furthermore, the vast majority of coupled-enzyme assays make use of redox enzymes that act on NAD/NADH, requiring absorbance changes to be monitored at 340 nm. This wavelength is suboptimal for the small assay volumes typical of HTS assays, where short path lengths and low extinction coefficients limit the signal window in a multi-well plate format [[23], [24], [25]]. Additionally, absorbance at 340 nm is subject to interference from small molecules, dust particles and standard assay components [23,25], resulting in an increased signal to noise ratio and an increased number of false positives.

To overcome the limitations associated with using coupled-enzyme assays, a novel 96-multi-well plate and fixed-time assay has been developed. The assay is based on the reaction of OAA, the product of the PC-catalyzed reaction, with Fast Violet B (FVB), a diazonium salt which produces a colored adduct with an absorbance maximum at 530 nm (Fig. 1). Diazonium salts have previously been used to detect OAA formation in other enzymatic systems such as phosphoenolpyruvate carboxylase and aspartate transaminase [[26], [27], [28], [29], [30]], but FVB has never been applied to determine PC activity. The assay readout is stable for an extended time period and accurately reports on enzyme activity from a single data point. The FVB fixed-time assay is reproducible, sensitive and responsive to known effectors of PC. The assay was used to screen a series of small molecule libraries that establishes it as an excellent primary assay for a concerted HTS program directed against PC.

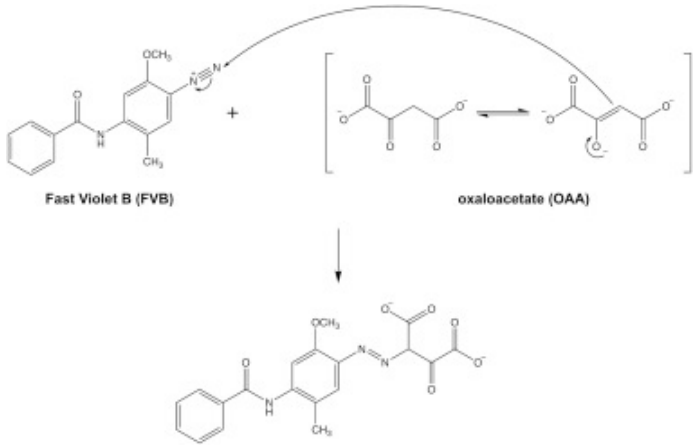

Fig. 1. Proposed mechanism for the reaction of oxaloacetate with Fast Violet B.

Materials and methods

Pyruvate carboxylase protein expression and purification

Rhizobium etli PC (*Re*PC) was co-expressed from a modified pET-17b-$(His)_9$ vector [31] with a pCY216 vector [32] encoding *E. coli* biotin protein ligase (*BirA*) in *E. coli* BL21Star(DE3) cells. *Staphylococcus aureus* PC (*Sa*PC) [33] and *Listeria monocytogenes* PC (*Lm*PC) were co-expressed from a pET-28a vector with a pCY216 vector in *E. coli* BL21Star(DE3) cells. *Re*PC, *Lm*PC and *Sa*PC were purified using Ni^{2+}-affinity and anion exchange chromatography as previously described [34]. In all cases, harvested cells were re-suspended in a lysis buffer containing 20 mM Tris (pH 7.8), 5 mM imidazole, 200 mM NaCl, 0.5 mM EGTA, 6 mM 2-mercaptoethanol, 300 µg/mL lysozyme, 1 mM phenylmethane-sulfonyl fluoride (PMSF), 1 µM pepstatin A, and 5 µM proteinase inhibior E−64. Cells were disrupted by sonication and the cell lysate was cleared by centrifugation at 4 °C prior to loading onto a 10 mL Ni^{2+}-NTA Profinity resin column (Bio-Rad Laboratories). The column was washed with 150 mL of lysis buffer followed by 150 mL of wash buffer (20 mM Tris; pH 7.8, 20 mM imidazole, 200 mM NaCl, 0.5 mM EGTA, 6 mM 2-mercaptoethanol). The *Re*PC enzyme was eluted from the column in elution buffer (20 mM Tris; pH 7.8, 250 mM imidazole, 200 mM NaCl, 0.5 mM EGTA, 6 mM 2-mercaptoethanol) with an 88 mL gradient of 20 mM imidazole wash buffer to 250 mM imidazole elution buffer. For *Sa*PC and *Lm*PC, the enzymes were eluted in a single step elution with 25–30 mL elution buffer.

All purified protein samples were pooled and dialyzed overnight in 1 L of Q-Sepharose buffer containing 20 mM triethanolamine (pH 8.0), 50 mM NaCl, 1 mM EGTA, and 2 mM DTT at 4 °C in preparation for anion exchange chromatography. Protein was loaded on a 10 mL column of Q-Sepharose Fast Flow resin (GE Healthcare) and the column was washed with 60 mL of Q-Sepharose buffer. The *Re*PC protein was eluted from the resin in Q-Sepharose buffer using a linear gradient from 50 mM to 1 M NaCl over 88 mL. For *Sa*PC and *Lm*PC, the enzymes were eluted in a single step elution with 25–30 mL of Q-sepharose buffer containing 1 M NaCl. Fractions were pooled and dialyzed against a storage buffer consisting of 10 mM Tris (pH 7.8), 150 mM KCl, 3 mM $MgCl_2$, 5% (v/v) glycerol and 2 mM DTT. An Amicon stirred cell with a 30,000-molecular weight cutoff filter was used to concentrate protein preparations to a range of 3–12 mg/mL. Concentrated protein was flash-frozen in liquid nitrogen prior to storage at −80 °C.

Preparation of assay reagents and solutions

All assay reagents and solutions were prepared separately and maintained at 22 °C for the full duration of the experiments. All substrates, effectors and enzyme were freshly dissolved and diluted in assay buffer containing 50 mM Bis-Tris (pH 7.7), 150 mM KCl, 3.0 mM $MgCl_2$, 0.5% triton X-100, and 1% DMSO. The final concentration of enzyme in the 100 µL enzymatic reaction was 10 µg/mL, except for *Lm*PC where the final concentration of enzyme in the 100 µL enzymatic reaction was 50 µg/mL. Where noted, oxalate and acetyl coenzyme A (Crystal Chem Inc., Elk Grove, IL) were included in the 100 µL enzymatic reaction at a final concentration of 5 mM and 0.25 mM, respectively. The substrate solution containing $NaHCO_3$, pyruvate and ATP was added to the 100 µL enzymatic reaction at a final concentration of

25 mM, 2 mM, and 1 mM, respectively. EDTA was prepared in assay buffer and served to inactivate the enzyme-catalyzed reaction at a final concentration of 12.7 mM. Fast Violet B Salt (FVB; Santa Cruz Biotechnology) was prepared at a stock concentration of 46 mM in DMSO. After vortexing the FVB stock solution to dissolve the dye, it was centrifuged at 9300 × g for 1 min and the clarified supernatant was separated from the salt pellet. The resulting FVB stock solution was protected from light exposure until it was introduced into the assay.

Assay procedures

For all experiments other than the evaluation of the Library of Pharmacologically Active Compounds (LOPAC, Sigma), 30 µL enzyme stock solution was added to each well in 96-well, flat bottom, polystyrene microplates (Santa Cruz Biotechnology) followed by the addition of 10 µL of the effectors (oxalate for inhibition, acetyl CoA for activation, assay buffer for the un-inhibited or un-activated reaction, and EDTA for measurement of the background signal). To initiate the enzyme-catalyzed reaction, 60 µL of a substrate stock solution containing pyruvate, HCO_3^- and ATP in assay buffer was added to each well. After 1 h, the enzyme reaction was inactivated by the addition of 10 µL of EDTA, followed by the addition of 10 µL of FVB to a final volume of 120 µL. The plates were sealed with microseal 'B' adhesive seals (Bio-Rad) and incubated for 2 h at 22 °C, prior to measuring absorbance values at 530 nm. All plates and reagents were maintained at 22 °C for the duration of the experiments. Reagents were dispensed using an automated liquid handling system (MultiFlo FX, Biotek) except for the effectors which were manually added using a hand-held, multi-channel micropipette. For the LOPAC screens, the procedure was slightly modified to incorporate a pintool (V&P Scientific) in combination with an Evo system (Tecan Life Sciences) to transfer the controls (0.4 µL) and compounds (0.2 µL) after the addition of enzyme. After the addition of the controls, 70 µL of the substrate stock solution was added to the wells to initiate the enzyme reaction.

Data analysis

The assay signal quality was statistically evaluated using the *Z*-factor value as described by Equation (1) [35], where σ_s and σ_c represent the standard deviations for the sample and control, respectively, and μ_s and μ_c represent the means for the sample and control, respectively.

$$Z = 1 - \frac{(3\sigma_s + 3\sigma_c)}{|\mu_s - \mu_c|} \quad (1)$$

To determine the agreement of the assay in measuring PC activity, the k_{cat} and K_M for pyruvate were determined by the following method: (1) An OAA standard curve was established to relate absorbance values at 530 nm to the OAA concentration. The standard curve was linear between 0 and 400 µM [OAA] (described in the results). (2) To determine the k_{cat} and K_M values using the FVB assay, the enzyme-catalyzed reaction at varying concentrations of pyruvate was inactivated at different time intervals. The absorbance values were then converted to [OAA] using the standard curve. Initial velocities ([OAA]/minute) were determined for each substrate concentration and plotted against pyruvate concentration. Equations (2), (3) were used to determine k_{cat} and K_M values, where $[E]_T$ represents the total enzyme

concentration, v_i represents initial velocity, V_{max} represents the maximum velocity and [S] represents the substrate concentration:

$$v_i = \frac{V_{max}[S]}{K_M+[S]} \quad (2)$$

$$k_{cat} = \frac{V_{max}}{[E]_T} \quad (3)$$

The validation experiments were designed and evaluated according to the recommendations of the “Assay Guidance Manual” from the National Center for Advancing Translational Sciences (NCATS), which includes all necessary pre-configured spreadsheets for analysis of the inter-plate and inter-day experiments [36].

For the LOPAC screen, percent activation and percent inhibition were calculated according to the equations (4), (5), where μ_C, μ_E and μ_R represent the means for the control (addition of acetyl CoA or oxalate), effector (screened small molecule), and reaction (the unaffected reaction), respectively:

$$\text{Percentactivation} = 100 - \left(\left(\frac{\mu_C-\mu_E}{\mu_C-\mu_R}\right) \times 100\right) \quad (4)$$

$$\text{Percentinhibition} = 100 - \left(\left(\frac{\mu_E-\mu_C}{\mu_R-\mu_C}\right) \times 100\right) \quad (5)$$

To determine the potency of specific effectors, the FVB assay was performed at varying effector concentrations. The dose-dependent response curves were evaluated using IC_{50} and EC_{50} equations, according to equation [6]:

$$Y = \frac{\text{bottom}+\text{top}-\text{bottom}}{1+10^{(\log IC_{50}-x)*\text{hillslope}}} \quad (6)$$

Curve fitting was performed using the software programs KaleidaGraph and Graphpad Prism.

Results

To accelerate the discovery of novel small molecule effectors of PC, it was necessary to establish an assay that can accurately measure PC activity in a high-throughput manner. Several diazonium salts have previously been utilized to detect OAA formation [26,27,29,30] but, to the best of our knowledge, they have never been applied to assay PC activity. Consequently, we sought to develop and validate a novel, fixed-time assay to measure PC activity via the formation of a colored adduct between the reaction product, OAA, and the diazonium salt, FVB.

FVB formed a colored adduct with OAA with an absorbance maximum at 530 nm, consistent with previously reported studies (Fig. 2A) [26,27]. None of the other assay components (HCO_3^-, pyruvate, ATP) contributed substantially to the absorbance at 530 nm in the presence of FVB, resulting in a large signal to noise ratio for OAA under all assay conditions. The absorbance at

530 nm was linear over a wide range of OAA concentrations between 1 and 400 μM, but deviated from linearity at OAA concentrations greater than ~400 μM (Fig. 2B). This deviation from linearity has previously been reported [26]. Because of this deviation, the accuracy of the assay is expected to decrease at concentrations of OAA in excess of 400 μM. As such, the assay was designed to maintain an upper limit of OD_{530} ~1 to maximize the signal window while ensuring accuracy. In this range, the assay is both reliable and sensitive in measuring OAA formation as a function of PC activity.

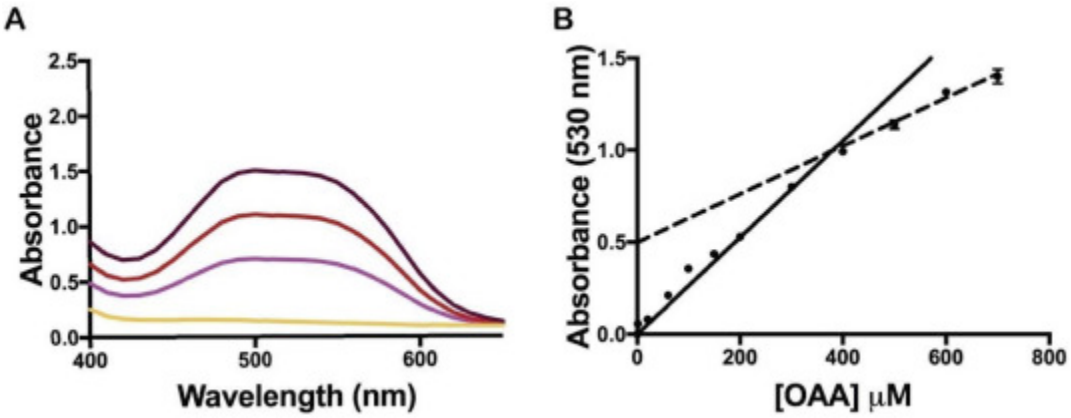

Fig. 2. Absorbance spectrum and OAA standard curve in the presence of 4 mM FVB. A) The background absorbance (yellow) in the assay was measured by the addition of the substrates (2.0 mM pyruvate, 1.0 mM ATP and 25 mM HCO_3^-) and assay buffer. The absorbance spectra recorded in assay buffer in the presence of substrates at varying concentrations of OAA are shown for 0.3 mM (pink), 0.6 mM (red) and 1.2 mM (purple) OAA. B) The absorbance (530 nm) of the FVB-OAA adduct responds linearly to OAA concentrations between 1 and 400 μM (solid line, $R^2 = 0.99$), while the dependence of absorbance on concentration begins to deviate from linearity at concentrations greater than 400 μM. This deviation can be approximated by a second standard curve between 400 and 800 μM (dashed line, $R^2 = 0.96$). Error bars represent the standard deviation from eight independent measurements. (For interpretation of the references to color in this figure legend, the reader is referred to the Web version of this article.)

An assay procedure was developed according to the schematic described in Fig. 3. Assay conditions were optimized for a 120 μL total reaction volume in a 96-well format. The assay comprises three overall steps: 1) a PC catalyzed reaction, 2) PC inactivation with EDTA, and 3) incubation with FVB. PC was first added to the wells, followed by the addition of the small molecule effector. The addition of the small molecules in this order facilitated the pre-incubation of the enzyme with effector molecules to account for potential slow-binding activators or inhibitors [21]. The enzymatic reaction was initiated by the addition of a large volume of substrates, to facilitate rapid and complete mixing in each well. EDTA was used to inactivate the reaction by chelating and sequestering the essential Mg^{2+} ions from the BC domain active site, immediately rendering the enzyme inactive [37] (Supplementary Figure S1). Previous studies have also demonstrated that EDTA assists in preventing diazonium salt precipitation [26]. Following enzyme inactivation, FVB was added and absorbance was measured at 530 nm following a 2 h incubation.

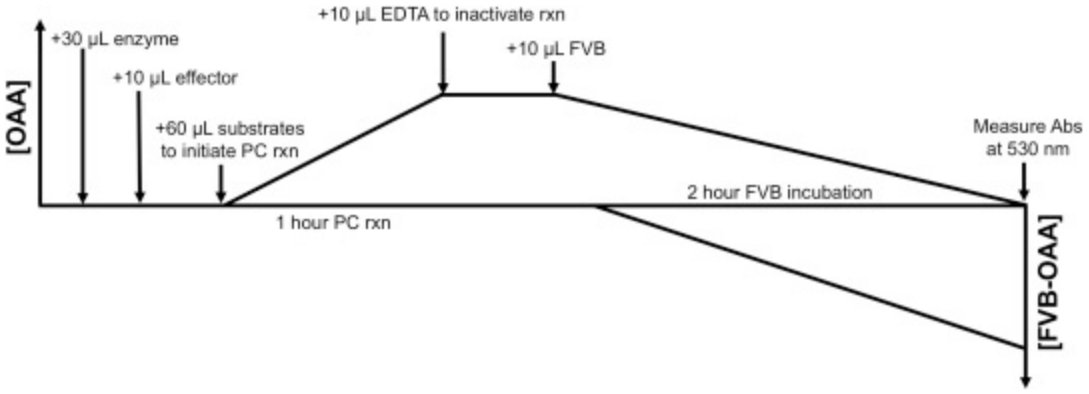

Fig. 3. 96-well fixed-time assay procedure. The PC-catalyzed reaction is initiated by the addition of substrates (2 mM pyruvate, 1 mM ATP, and 25 mM $NaHCO_3$). After 1 h, the PC-catalyzed reaction is inactivated by the addition of 12.7 mM EDTA. FVB is subsequently added to a final concentration of 4 mM for 2 h prior to reading the absorbance of the FVB-OAA colored adduct at 530 nm. This procedure can be performed manually or with an automated liquid handling system.

To test the ability of the assay to detect activators and inhibitors of PC, the assay procedure was validated by measuring the absorbance of the colored FVB-OAA adduct in the presence of acetyl CoA (activator) and oxalate (inhibitor). The activator and inhibitor were used to test the reliability and signal window of the assay as a prerequisite for its application in small molecule dose-dependent measurements. The background reaction was measured in the presence of inactivating EDTA and resulted in similar absorbance values (~0.2 Abs) as the inhibited reaction in the presence of 5 mM oxalate. The activated reaction in the presence of 0.25 mM acetyl CoA resulted in an increase in absorbance (~1.0–1.2 Abs) when compared to the unaltered reaction without any small molecule effectors added (~0.5–0.6 Abs). The EC_{50} value for acetyl CoA (45 µM) and the IC_{50} value for oxalate (97 µM) were determined for *Re*PC (Fig. 4). These values are consistent with published K_A and K_D values of 10 µM and 130 µM, respectively, thus further confirming the reliability of this method [38,39]. These results strongly support that the FVB assay can be simultaneously utilized to screen for both activators and inhibitors of PC in a HTS program.

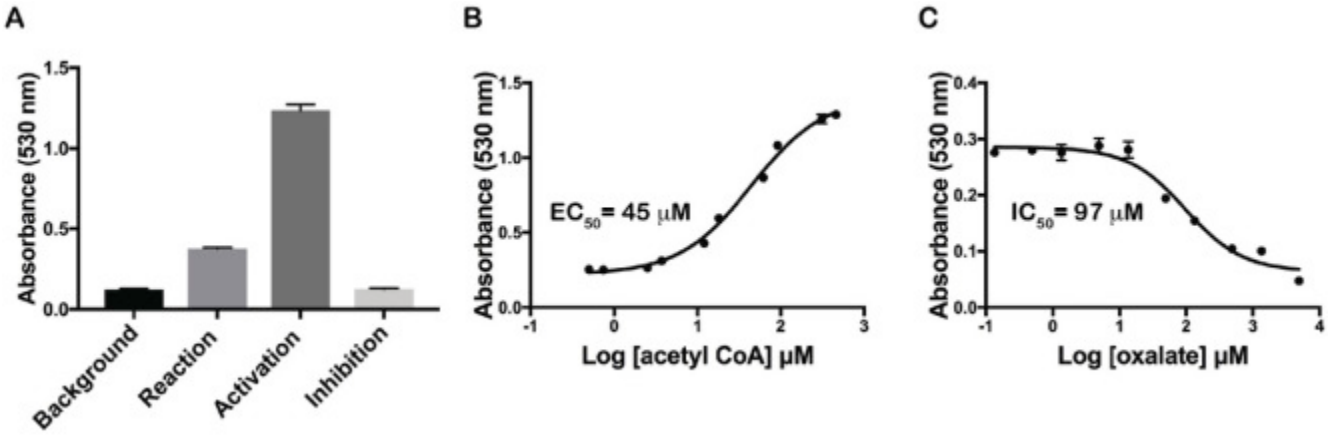

Fig. 4. FVB assay optimization and dose dependent response with known effectors of *Re*PC. A) The primary assay method was evaluated in the presence of established effectors of PC activity. The “background” signal was

determined from the reaction of PC in the presence of 12.7 mM EDTA. The “reaction” signal was determined from the reaction of PC in the absence of any effectors. The “activation” signal was determined from the reaction of PC in the presence of the activator, acetyl CoA (0.25 mM). The “inhibition” signal was determined from the reaction of PC in the presence of the inhibitor, oxalate (5 mM). The differences between the group means were statistically significant, as determined by one-way ANOVA ($F(3, 28) = 5956$, $p < 0.0001$). B) Titration of acetyl CoA gives an EC_{50} value for acetyl CoA of 45 µM. C) Titration of oxalate gives an IC_{50} value for oxalate of 97 µM. In all plots, error bars represent the standard deviation from eight independent measurements.

To further assess the reliability of this assay, steady-state kinetic constants were determined for *Rhizobium etli* PC (*Re*PC). *Re*PC has been extensively structurally and kinetically characterized in the presence of both oxalate and acetyl-CoA, serving as an ideal model system for validation. The K_M value for pyruvate (1.5 ± 0.3 mM) and the k_{cat} value (120 ± 20 min^{-1}) were determined for *Re*PC (Supplementary Figure S2) and are consistent with previously reported values [40,41].

Assays that are transitioned to HTS need to not only be reliable, accurate and sensitive but also robust, reproducible and statistically validated [35]. To assess the quality of the assay to be transitioned to a HTS platform, PC was statistically evaluated in the presence of both acetyl CoA and oxalate. *Z*-factors can be utilized to compare, evaluate and validate the suitability of an assay for HTS. A *Z*-factor score of 0.5–1.0 indicates that the assay has a high dynamic range and low variation in the signal measurements and is an excellent assay. *Z′*-factors are used to determine the overall quality of the assay without interference from small molecule effectors. Alternatively, *Z*-factors take into account the signal separation and error of the assay when used with small molecule activators or inhibitors. In order to determine the robustness and quality of the assay, *Z*-factors and *Z′*-factors were calculated for *Re*PC, *Listeria monocytogenes* PC (*Lm*PC) and *Staphylococcus aureus* PC (*Sa*PC) (Table 1). PC enzymes from multiple source organisms were selected to determine the suitability of various bacterial PC enzymes for HTS. The excellent *Z*-factors for *Re*PC, *Lm*PC and *Sa*PC demonstrate that this assay is amenable to high-throughput screening for both activators and inhibitors of PC enzymes from a range of organisms. The results suggest, however, that assay conditions must be individually optimized for PC enzymes from different species, as demonstrated by the increased enzyme concentration (50 µg/mL) required to obtain high *Z*-factors in the assay catalyzed by *Lm*PC.

Table 1. Z- Factors Determined for the assay of bacterial PC enzymes.

PC Origin	Enzyme [ ] µg/mL	Z′-Factor	Z-Factor Activation	Z-Factor Inhibition	Assay Score
Rhizobium etli	10	0.86	0.85	0.87	Excellent
Listeria monocytogenes	50	0.70	0.77	0.70	Excellent
Staphylococcus aureus	10	0.87	0.87	0.87	Excellent

In consideration of using this assay in a HTS context, a series of additional optimization and validation tests were performed using automatic liquid dispensing protocols. Most small molecules from screening libraries are dissolved in DMSO and are added at fixed concentrations in the screening assays. Thus, it was necessary to evaluate the tolerance of PC for DMSO [36]. PC activity was not affected by the presence of 1% DMSO (Supplementary

Figure S3). Additionally, all reagents were stable at 22 °C for up to 8 h, and the final measured absorbance values were stable between 2 and 5 h of incubation with FVB (Fig. 5). A three-day plate uniformity assessment using the interleaved-signal format [36] was performed in the presence of the inhibitor, oxalate. This demonstrated that the signal windows, *Z*-factors and spatial uniformity meet all criteria for consistent plate readouts across multiple plates and days (Fig. 6A). A two-day validation test was performed for activation in the presence of acetyl CoA, demonstrating consistent plate readouts across multiple plates and days (Fig. 6B; Supplementary Table S1).

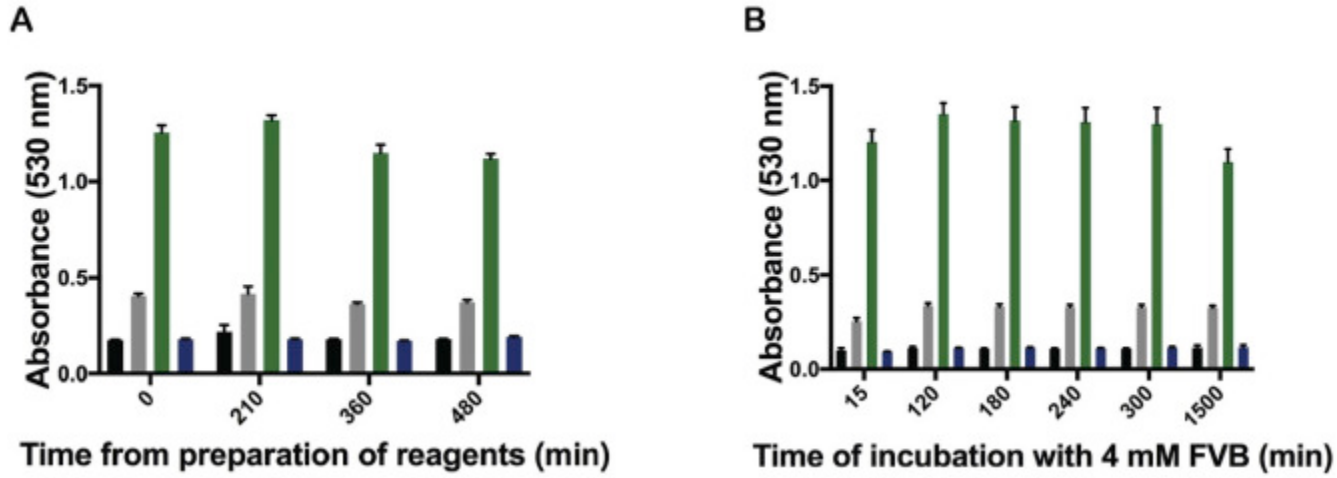

Fig. 5. Reagent and signal stability for the FVB-based assay. In all plots, the background signal (black) represents the inactivated PC reaction in the presence of 12.7 mM EDTA. The reaction signal (grey) represents the PC reaction in the absence of effectors. The activation signal (green) represents the PC reaction in the presence of the activator, acetyl-CoA (0.25 mM). The inactivation signal (blue) represents the PC reaction in the presence of the inhibitor, oxalate (5 mM). A) All reagents used in the FVB-based assay are stable under all conditions for up to 8 h at 22 °C. The first assay was run at time zero with freshly prepared reagents. These same reagents were used for all subsequent reactions, yielding consistent measurements for up to 480 min beyond the time of the first assay. B) Incubation times between 120 and 300 min yield consistent absorbance measurements, indicating that the FVB-OAA color adduct is stable for an extended time period, permitting the measurement of plates at any time between 2 and 5 h post-incubation with FVB. In both plots, error bars represent the standard deviation from eight independent measurements. (For interpretation of the references to color in this figure legend, the reader is referred to the Web version of this article.)

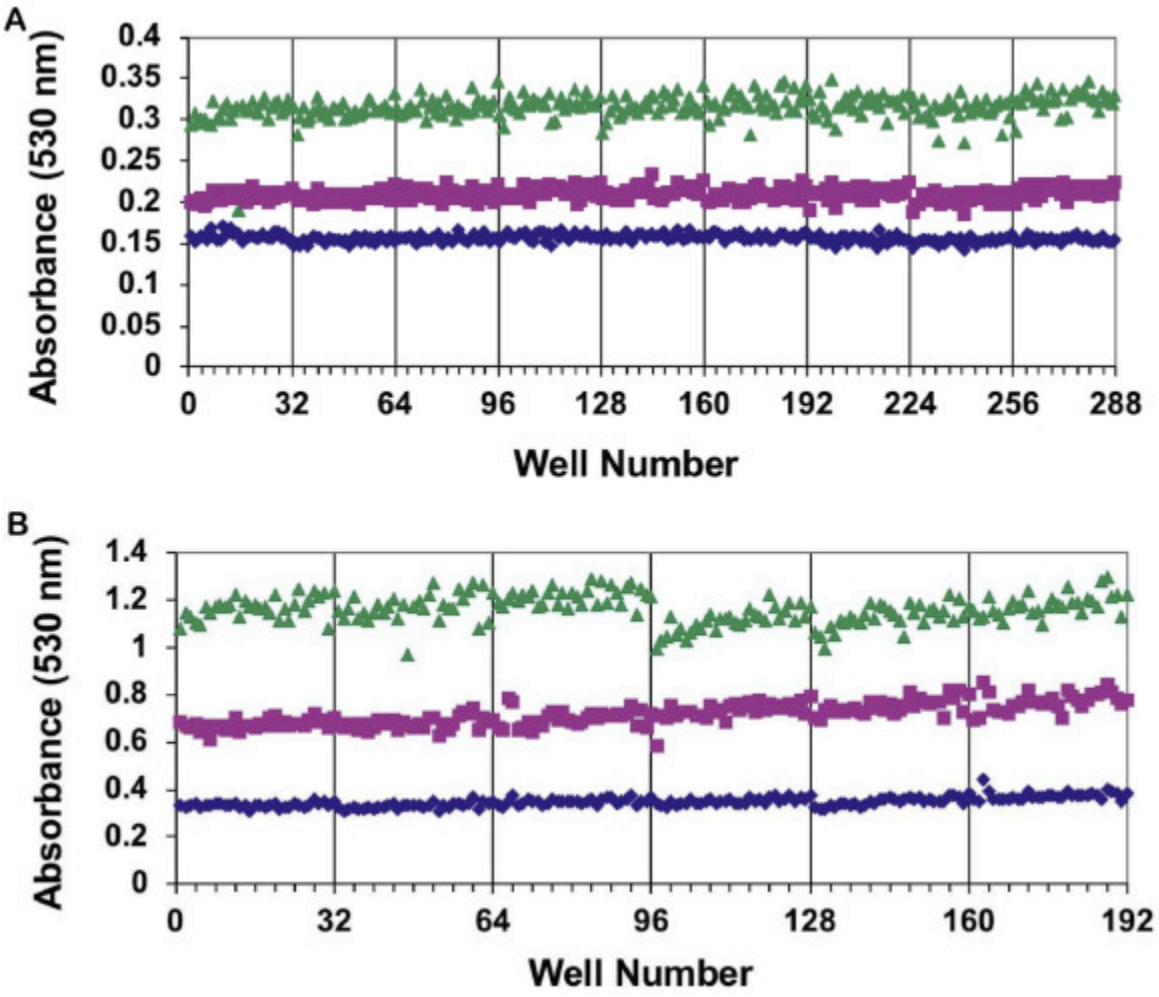

Fig. 6. Plate uniformity validation tests for *Re*PC with oxalate and acetyl-CoA. Both plate uniformity tests reveal consistent signals across all plates and across multiple days. Well number 0–96, 97–192 and 193–288 refer to Day 1, Day 2 and Day 3, respectively. No edge or drift effects were observed and all statistical measures are acceptable. A) 3-day inhibition plate uniformity assessment with 5 mM oxalate for the minimal signal (blue diamonds), 90 μM oxalate for the IC_{50} signal (pink squares) and the uninhibited PC reaction for the maximal signal (green triangles). B) 2-day activation plate uniformity assessment with 250 μM acetyl-CoA as the maximal signal (green triangles), 50 μM acetyl-CoA for the EC_{50} signal (pink squares) and the uninhibited PC reaction as the minimal signal (blue diamonds). (For interpretation of the references to color in this figure legend, the reader is referred to the Web version of this article.)

The FVB assay was used to screen *Re*PC against a LOPAC library (Library of Pharmacologically Active Compounds, Sigma) to validate the responsiveness of the assay to a library of well-characterized bioactive compounds. *Re*PC was screened against the LOPAC library on three separate occasions and reproducibly identified two inhibitors in all three iterations of the screen (Fig. 7). Consistent activation and inhibition signals were obtained for individual plate controls across all 16 plates and all plates had excellent *Z*-factors (Fig. 7A and B). The screen identified two compounds that resulted in 70–91% inhibition (Fig. 7D). The two hit compounds, cisplatin and pyriplatin, were confirmed by dose-dependent response assays, yielding IC_{50} values of 22 μM and 30 μM, respectively (Fig. 8). While the steep dose-response curve for these compounds suggests that they are likely acting as non-specific alkylating

agents [42,43] or promiscuous aggregators [44], the results from the pilot screen nevertheless indicate that the assay can reproducibly and reliably identify an appropriate number of potential inhibitor hit compounds. The LOPAC pilot screen did not identify any potential activators for *Re*PC, indicating that a larger, more diverse library is required to identify activators (Fig. 7C). All optimization and validation results indicate that the assay is reproducible, reliable and sufficiently sensitive to detect a range of small molecule effectors of PC within screening libraries.

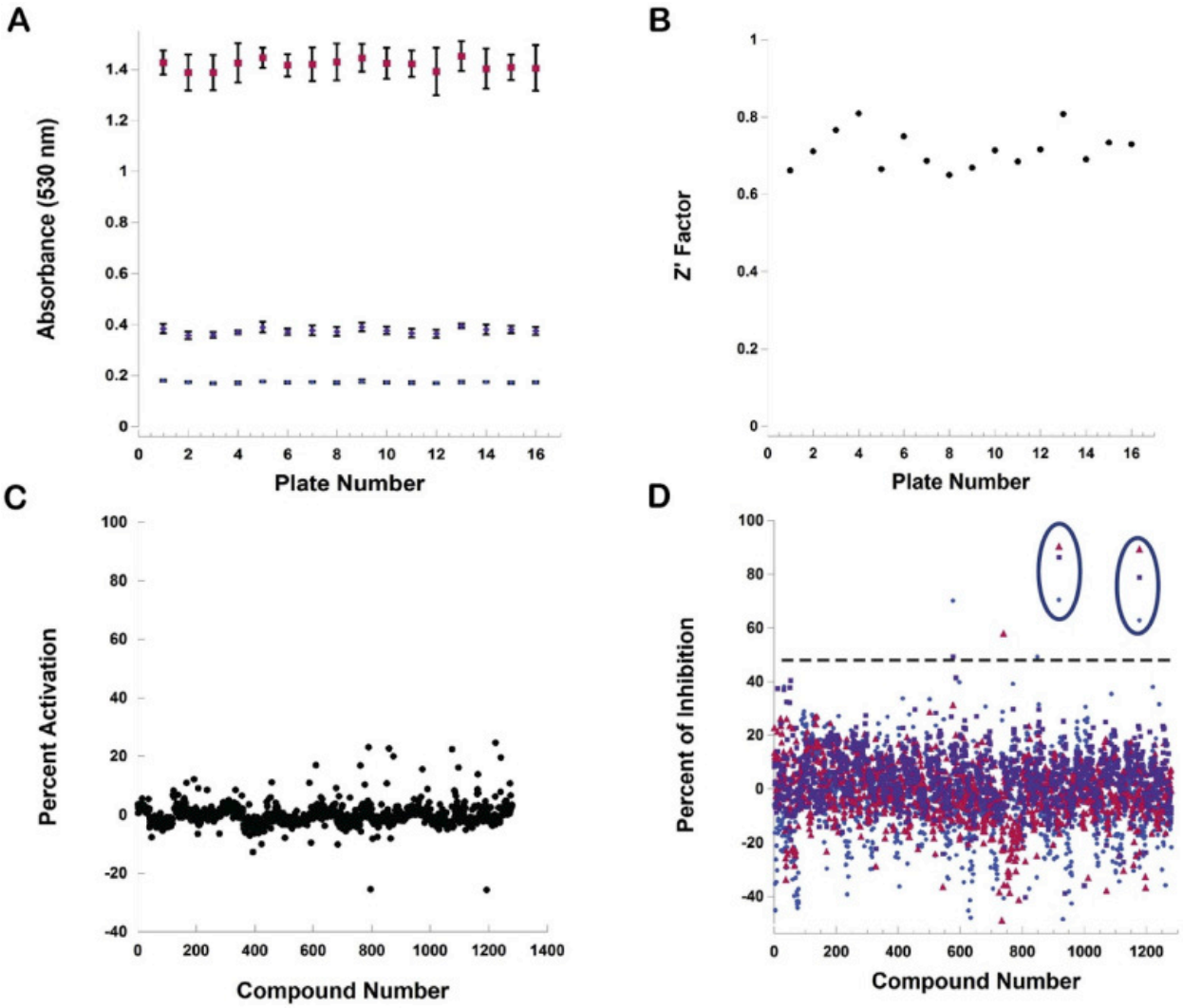

Fig. 7. LOPAC (Library of Pharmacologically Active Compounds) screen results for inhibitors and activators of *Rhizobum etli* PC. A) Absorbance signals for individual plate controls. The maximal signal is determined in the presence of 250 μM acetyl-CoA (pink squares), the normal PC reaction is determined in the absence of effectors (purple squares) and the inhibited reaction is determined in the presence of 5 mM oxalate (blue squares). Error bars represent the standard deviation from eight independent measurements. B) *Z*-factors fall in a range considered to be excellent (0.6–0.8) and are consistent across all 16 plates. C) Percent of activation from Screen 1 of the LOPAC screen D) Combined inhibition data from three individual LOPAC screens (Screen 1, blue; Screen 2, pink; and Screen 3, purple). The dashed line represents a threshold of 3× the standard deviation for the combined data, equivalent to 45% inhibition. Two compounds consistently exceeded this threshold across all

three screens. (For interpretation of the references to color in this figure legend, the reader is referred to the Web version of this article.)

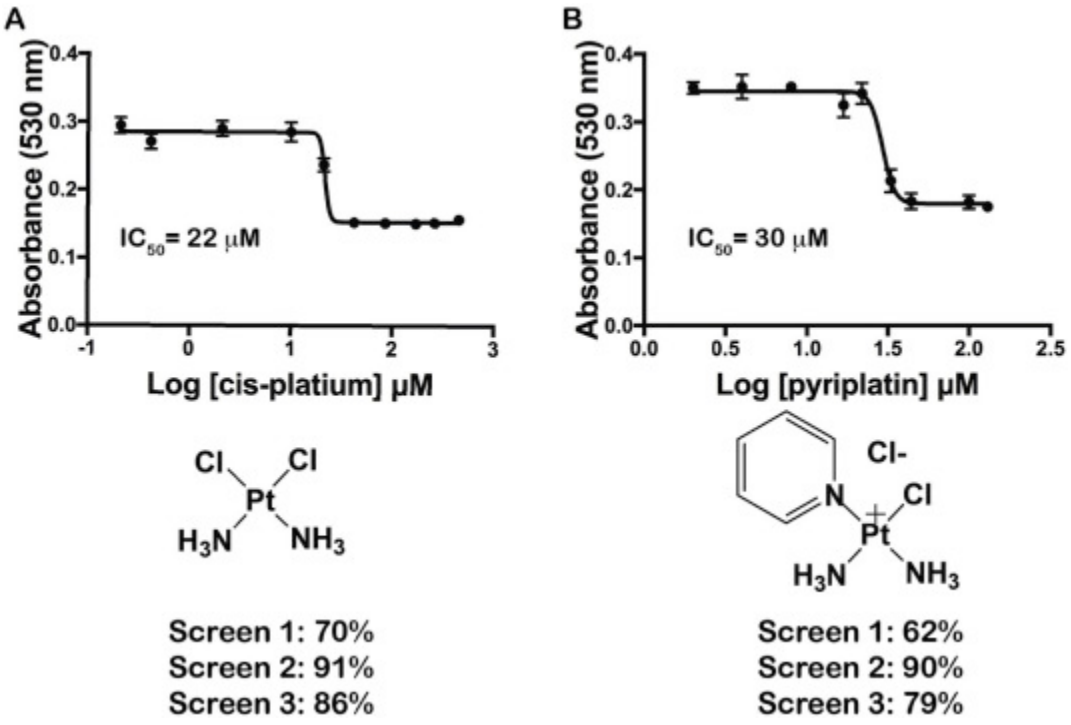

Fig. 8. Dose dependent response for the two inhibitors, cisplatin and pyriplatin, identified in the LOPAC screen. A) Dose-dependent response for the inhibition of *R. etli* PC in the presence of cisplatin results in an IC_{50} value of 22 μM. B) Dose-dependent response for the inhibition of *R. etli* PC in the presence of pyriplatin results in an IC_{50} value of 30 μM. The chemical structures of the hit compounds and the percent of inhibition measured in each of the three independent screens are indicated. In both plots, error bars represent the standard deviation from eight independent measurements.

Discussion

A novel, fixed time assay for PC has been developed that is reliable, sensitive and robust. The assay monitors the production of OAA through the formation of a colored adduct between OAA and the commercially available diazonium salt of FVB. This offers a simple assay to detect PC activity through monitoring an increase in absorbance at 530 nm. The assay can be utilized as an alternative method to coupled-enzyme assays for the detection of PC activity. Additionally, the assay can readily be transitioned to a multi-well plate format where the reagent stability, accuracy and reproducibility is ideal for use in high-throughput screening of small molecule libraries for both activators and inhibitors of PC activity.

While diazonium salts have previously been used to detect the production of OAA, they have not specifically been applied to assay PC activity. Diazonium salts such as Fast Red KL, Fast Ponceau L and Fast Violet B have been used to detect OAA production from aspartate transaminase [26,28,45,46]. Fast Violet B, in particular, has also been utilized to assess phosphoenolpyruvate carboxylase activity and has previously been optimized in a microtiter plate assay [27,29]. The choice of Fast Violet B over other diazonium salts in this assay is based

on several factors. Fast Violet B is stable over a pH range of 7.0–7.5 and tolerates the addition of both EDTA and detergent [27,28,45,47]. Conversely, Fast Red KL and Fast Ponceau L were most stable over a pH range of 4.2–4.6 [26,28,45,46]. Additionally, Fast Violet B has a broad absorption peak between 490 and 540 nm compared to the narrower absorption peaks of Fast Red KL and Fast Ponceau L (455–467 nm respectively), enabling greater flexibility in the assay parameters [26,28]. The red-shifted absorbance wavelength of FVB also reduces the likelihood of interference with small molecule effectors. Lastly, FVB has previously been used in a microtiter plate-based assay for phosponenolpyruvate carboxylase, indicating that it is amenable to the smaller reaction volumes typical of a high throughput screening assay.

The FVB-based assay is capable of accurately measuring steady state kinetics in PC, consistent with a study by Amador and Salvatore (1971) that compared the activity of aspartate aminotransferase measured by FVB and Fast Ponceau L to the rates determined by a MDH coupled-enzyme assay. Thus, the FVB fixed-time assay can be employed as an alternative to the MDH coupled-enzyme assay for standard kinetic measurements of PC activity in instances where assay conditions interfere with the coupling enzyme. For example, many α-keto acids serve as inhibitors of PC [38] but MDH has been shown to reduce aromatic α-keto acids [48], precluding careful inhibition studies using the standard MDH coupled enzyme assay. The FVB-based enzyme assay is free of secondary coupling enzymes that might otherwise be subject to cross-reactivity and, as such, represents an important and complementary tool for detailed kinetic studies of PC. It must be noted that the reaction times employed for measuring initial velocity kinetics (0–60 s; Supplementary Figure S2) are substantially different from the reaction time that is employed in the high throughput screening applications (1 h; Fig. 4, Fig. 5, Fig. 6). In high throughput screening, a 1 h enzyme-catalyzed reaction produces an ideal signal window for screening PC effectors, despite deviating from initial velocity conditions. Thus, the enzyme reaction times must be selected to coincide with the assay objectives: 1 h for high throughput screening vs. 10–60 s for measuring initial velocity kinetics.

While it has many advantages, the FVB assay also has certain limitations that must be carefully considered. FVB, like all diazonium salts, has the potential for cross-reactivity with nucleophilic compounds. For example, it has previously been demonstrated that FVB forms a colored adduct with α-ketoglutarate [26] and occasionally produced false positives due to ketosis in serums [46]. Additionally, FVB reacts with high concentrations (>250 μM) of acetyl CoA and CoA, resulting in a decrease in the FVB-OAA adduct (Supplementary Figure S4). Thus, small molecule activators may be difficult to identify if their interference with FVB-OAA colored adduct formation offsets their enhancement of PC activity. This may be one reason why PC activators were not observed in the LOPAC screen. It is also likely, however, that it is simply more difficult to find activators of PC, as allosteric ligands are generally more difficult to detect by HTS [49].

Lastly, consideration should be given to determining the appropriate concentration of substrates to be used in the FVB assay, particularly where it is being applied as a HTS primary screen. Here, the assay has been performed at 2 mM pyruvate, which is less than the saturating concentrations of 5–20 mM pyruvate, depending on the source of the PC enzyme. This sub-saturating concentration of pyruvate maximizes the signal to noise ratio of the assay

for *Re*PC but, notably, has not been optimized for *Lm*PC or *Sa*PC. The substrate concentrations in a HTS assay will influence the detection of weak inhibitors [22,50]. It was determined by Yang et al. that performing inhibitor screens at substrate concentrations near to the K_M value is ideal to detect competitive, non-competitive and uncompetitive inhibitors [50]. Thus, prior to embarking on a detailed HTS program, it will be important to consider the substrate concentrations in relation to the K_M values of the substrates, particularly if certain types of inhibitors (i.e. competitive vs. non-competitive) are being sought against a PC target from a desired organism.

In conclusion, a novel, fixed-time assay to detect PC activity has been established. This assay can be used to screen for small molecule effectors of PC or as an alternative method to measure steady state enzyme kinetics. The development and validation of this assay will enable future HTS for the discovery of small molecule effectors of PC. The resulting small molecules that will be discovered and developed using this assay will have great potential as biochemical tools to further investigate the regulation and structure of PC, as well as the metabolic role that it plays in infection and disease.

Appendix A. Supplementary data

The following is the supplementary data related to this article:

Download Acrobat PDF file (785KB)Help with pdf files

Multimedia component 1.

References

[1] S. Jitrapakdee, M. St Maurice, I. Rayment, W.W. Cleland, J.C. Wallace, P.V. Attwood**Structure, mechanism and regulation of pyruvate carboxylase**, Biochem. J., 413 (2008), pp. 369-387

[2] S. Jitrapakdee, A. Vidal-Puig, J.C. Wallace**Anaplerotic roles of pyruvate carboxylase in mammalian tissues**, Cell. Mol. Life Sci., 63 (2006), pp. 843-854

[3] T. Cheng, J. Sudderth, C. Yang, A.R. Mullen, E.S. Jin, J.M. Mates, R.J. DeBerardinis**Pyruvate carboxylase is required for glutamine-independent growth of tumor cells**, Proc. Natl. Acad. Sci. U. S. A., 108 (2011), pp. 8674-8679

[4] S. Christen, D. Lorendeau, R. Schmieder, D. Broekaert, K. Metzger, K. Veys, I. Elia, J.M. Buescher, M.F. Orth, S.M. Davidson, T.G. Grunewald, K. De Bock, S.M. Fendt**Breast cancer-derived lung metastases show increased pyruvate carboxylase-dependent anaplerosis**, Cell Rep., 17 (2016), pp. 837-848

[5] S. Farfari, V. Schulz, B. Corkey, M. Prentki**Glucose-regulated anaplerosis and cataplerosis in pancreatic beta-cells: possible implication of a pyruvate/citrate shuttle in insulin secretion**, Diabetes, 49 (2000), pp. 718-726

[6] M.V. Jensen, J.W. Joseph, O. Ilkayeva, S. Burgess, D. Lu, S.M. Ronnebaum, M. Odegaard, T.C. Becker, A.D. Sherry, C.B. Newgard**Compensatory responses to pyruvate**

carboxylase suppression in islet beta-cells. Preservation of glucose-stimulated insulin secretion, J. Biol. Chem., 281 (2006), pp. 22342-22351

[7] P. Phannasil, C. Thuwajit, M. Warnnissorn, J.C. Wallace, M.J. MacDonald, S. Jitrapakdee**Pyruvate carboxylase is up-regulated in breast cancer and essential to support growth and invasion of MDA-MB-231 cells**, PLoS One, 10 (2015), e0129848

[8] J. Schar, R. Stoll, K. Schauer, D.I. Loeffler, E. Eylert, B. Joseph, W. Eisenreich, T.M. Fuchs, W. Goebel**Pyruvate carboxylase plays a crucial role in carbon metabolism of extra- and intracellularly replicating Listeria monocytogenes**, J. Bacteriol., 192 (2010), pp. 1774-1784

[9] J. Xu, J. Han, Y.S. Long, P.N. Epstein, Y.Q. Liu**The role of pyruvate carboxylase in insulin secretion and proliferation in rat pancreatic beta cells**, Diabetologia, 51 (2008), pp. 2022-2030

[10] U. Lao-On, P.V. Attwood, S. Jitrapakdee**Roles of pyruvate carboxylase in human diseases: from diabetes to cancers and infection**, J. Mol. Med. (Berl.), 96 (2018), pp. 237-247

[11] N.M. Hasan, M.J. Longacre, S.W. Stoker, T. Boonsaen, S. Jitrapakdee, M.A. Kendrick, J.C. Wallace, M.J. MacDonald**Impaired anaplerosis and insulin secretion in insulinoma cells caused by small interfering RNA-mediated suppression of pyruvate carboxylase**, J. Biol. Chem., 283 (2008), pp. 28048-28059

[12] A.T. Whiteley, N.E. Garelis, B.N. Peterson, P.H. Choi, L. Tong, J.J. Woodward, D.A. Portnoy**c-di-AMP modulates Listeria monocytogenes central metabolism to regulate growth, antibiotic resistance and osmoregulation**, Mol. Microbiol., 104 (2017), pp. 212-233

[13] K. Sureka, P.H. Choi, M. Precit, M. Delince, D.A. Pensinger, T.N. Huynh, A.R. Jurado, Y.A. Goo, M. Sadilek, A.T. Iavarone, J.D. Sauer, L. Tong, J.J. Woodward**The cyclic dinucleotide c-di-AMP is an allosteric regulator of metabolic enzyme function**, Cell, 158 (2014), pp. 1389-1401

[14] T.N. Zeczycki, M. St. Maurice, P.V. Attwood**Inhibitors of pyruvate carboxylase**, Open Enzym. Inhib. J., 3 (2010), pp. 8-26

[15] P.H. Choi, T.M.N. Vu, H.T. Pham, J.J. Woodward, M.S. Turner, L. Tong**Structural and functional studies of pyruvate carboxylase regulation by cyclic di-AMP in lactic acid bacteria**, Proc. Natl. Acad. Sci. U. S. A., 114 (2017), pp. E7226-e7235

[16] H.P. Makkar, P. Siddhuraju, K. Becker**Plant secondary metabolites**, Meth. Mol. Biol., 393 (2007), pp. 1-122

[17] W.B. Novoa, A.D. Winer, A.J. Glaid, G.W. Schwert**Lactic dehydrogenase. V. inhibition by oxamate and by oxalate**, J. Biol. Chem., 234 (1959), pp. 1143-1148

[18] D.B. Northrop, H.G. Wood**Transcarboxylase. VII. exchange reactions and kinetics of oxalate inhibition**, J. Biol. Chem., 244 (1969), pp. 5820-5827

[19] T.N. Zeczycki, A.L. Menefee, A. Adina-Zada, S. Jitrapakdee, K.H. Surinya, J.C. Wallace, P.V. Attwood, M. St Maurice, W.W. Cleland**Novel insights into the biotin carboxylase domain reactions of pyruvate carboxylase from *Rhizobium etli***, Biochemistry, 50 (2011), pp. 9724-9737

[20] P.V. Attwood, W.W. Cleland**Decarboxylation of oxalacetate by pyruvate carboxylase**, Biochemistry, 25 (1986), pp. 8191-8196
[21] J.F. Glickman**Assay development for protein kinase enzymes**, G.S. Sittampalam, N.P. Coussens, K. Brimacombe, A. Grossman, M. Arkin, D. Auld, C. Austin, J. Baell, B. Bejcek, T.D.Y. Chung, J.L. Dahlin, V. Devanaryan, T.L. Foley, M. Glicksman, M.D. Hall, J.V. Hass, J. Inglese, P.W. Iversen, S.D. Kahl, S.C. Kales, M. Lal-Nag, Z. Li, J. McGee, O. McManus, T. Riss, O.J. Trask Jr., J.R. Weidner, M. Xia, X. Xu (Eds.), Assay Guidance Manual, Eli Lilly & Company and the National Center for Advancing Translational Sciences, Bethesda (MD) (2004)
[22] M.G. Acker, D.S. Auld**Considerations for the design and reporting of enzyme assays in high-throughput screening applications**, Perspect. Sci., 1 (2014), pp. 56-73
[23] J. Inglese, R.L. Johnson, A. Simeonov, M. Xia, W. Zheng, C.P. Austin, D.S. Auld**High-throughput screening assays for the identification of chemical probes**, Nat. Chem. Biol., 3 (2007), pp. 466-479
[24] A. Simeonov, M.I. Davis**Interference with fluorescence and absorbance**, G.S. Sittampalam, N.P. Coussens, K. Brimacombe, A. Grossman, M. Arkin, D. Auld, C. Austin, J. Baell, B. Bejcek, T.D.Y. Chung, J.L. Dahlin, V. Devanaryan, T.L. Foley, M. Glicksman, M.D. Hall, J.V. Hass, J. Inglese, P.W. Iversen, S.D. Kahl, S.C. Kales, M. Lal-Nag, Z. Li, J. McGee, O. McManus, T. Riss, O.J. Trask Jr., J.R. Weidner, M. Xia, X. Xu (Eds.), Assay Guidance Manual, Eli Lilly & Company and the National Center for Advancing Translational Sciences, Bethesda (MD) (2004)
[25] A. Simeonov, A. Jadhav, A.A. Sayed, Y. Wang, M.E. Nelson, C.J. Thomas, J. Inglese, D.L. Williams, C.P. Austin**Quantitative high-throughput screen identifies inhibitors of the *Schistosoma mansoni* redox cascade**, PLoS Neglected Trop. Dis., 2 (2008), p. e127
[26] S.M. Sax, J.J. Moore**Determination of glutamic oxalacetic transaminase activity by coupling of oxalacetate with diazonium salts**, Clin. Chem., 13 (1967), pp. 175-185
[27] W. Cockburn, G.C. Whitelam, S.P. Slocombe, R.A. McKee**A microtiter plate-based assay for phosphoenolpyruvate carboxylase**, Anal. Biochem., 189 (1990), pp. 95-98
[28] A.J. Lombarts, H.J. Peters**An improved automated assay of serum glutamic-oxalacetic transaminase**, Clin. Chim. Acta, 35 (1971), pp. 257-264
[29] K.A. Norris, A.R. Atkinson, W.G. Smith**Colorimetric enzymatic determination of serum total carbon dioxide, as applied to the Vickers Multichannel 300 discrete analyzer**, Clin. Chem., 21 (1975), pp. 1093-1101
[30] A.L. Babson, P.O. Shapiro, P.A. Williams, G.E. Phillips**The use of a diazonium salt for the determination of glutamic-oxalacetic transaminase in serum**, Clin. Chim. Acta, 7 (1962), pp. 199-205
[31] A. Chapman-Smith, D.L. Turner, J.E. Cronan Jr., T.W. Morris, J.C. Wallace**Expression, biotinylation and purification of a biotin-domain peptide from the biotin carboxy Carrier protein of Escherichia coli acetyl-CoA carboxylase**, Biochem. J., 302 (Pt 3) (1994), pp. 881-887

[32] M. St Maurice, L. Reinhardt, K.H. Surinya, P.V. Attwood, J.C. Wallace, W.W. Cleland, I. Rayment**Domain architecture of pyruvate carboxylase, a biotin-dependent multifunctional enzyme**, Science, 317 (2007), pp. 1076-1079

[33] S. Xiang, L. Tong**Crystal structures of human and Staphylococcus aureus pyruvate carboxylase and molecular insights into the carboxyltransfer reaction**, Nat. Struct. Mol. Biol., 15 (2008), pp. 295-302

[34] A.D. Lietzan, A.L. Menefee, T.N. Zeczycki, S. Kumar, P.V. Attwood, J.C. Wallace, W.W. Cleland, M. St Maurice**Interaction between the biotin carboxyl Carrier domain and the biotin carboxylase domain in pyruvate carboxylase from *Rhizobium etli***, Biochemistry, 50 (2011), pp. 9708-9723

[35] J.H. Zhang, T.D. Chung, K.R. Oldenburg**A simple statistical parameter for use in evaluation and validation of high throughput screening assays**, J. Biomol. Screen, 4 (1999), pp. 67-73

[36] G. Sittampalam, N. Coussens, K. Brimacombe, *et al.***HTS assay validation**, Assay Guidance Manual [Internet], Eli Lilly & Company and the National Center for Advancing Translational Sciences, Bethesda (MD) (2012)

[37] S.A. Osmani, M.C. Scruton (Ed.), The Effect of EDTA on the Apparent Hysteretic Properties of Pyruvate Carboxylase from *Rhizopus arrhizus*, FEBS Letters (1984), pp. 157-160

[38] A.D. Lietzan, M. St Maurice**Insights into the carboxyltransferase reaction of pyruvate carboxylase from the structures of bound product and intermediate analogs**, Biochem. Biophys. Res. Commun., 441 (2013), pp. 377-382

[39] A. Adina-Zada, T.N. Zeczycki, P.V. Attwood**Regulation of the structure and activity of pyruvate carboxylase by acetyl CoA**, Arch. Biochem. Biophys., 519 (2012), pp. 118-130

[40] T.N. Zeczycki, A.L. Menefee, S. Jitrapakdee, J.C. Wallace, P.V. Attwood, M. St Maurice, W.W. Cleland**Activation and inhibition of pyruvate carboxylase from *Rhizobium etli***, Biochemistry, 50 (2011), pp. 9694-9707

[41] T.N. Zeczycki, M. St Maurice, S. Jitrapakdee, J.C. Wallace, P.V. Attwood, W.W. Cleland**Insight into the carboxyl transferase domain mechanism of pyruvate carboxylase from *Rhizobium etli***, Biochemistry, 48 (2009), pp. 4305-4313

[42] J.L. Pujol, L. Carestia, J.P. Daurès**Is there a case for cisplatin in the treatment of small-cell lung cancer? a meta-analysis of randomized trials of a cisplatin-containing regimen versus a regimen without this alkylating agent**, Br. J. Cancer, 83 (2000), pp. 8-15

[43] L.F. Porrata, A.A. Adjei**The pharmacologic basis of high dose chemotherapy with haematopoietic stem cell support for solid tumours**, Br. J. Cancer, 85 (2001), pp. 484-489

[44] B.K. Shoichet**Interpreting steep dose-response curves in early inhibitor discovery**, J. Med. Chem., 49 (2006), pp. 7274-7277

[45] A.L. Babson, P.O. Shapiro, P.A.R. Williams, G.E. Phillips**The use of a diazonium salt for the determination of glutamic-oxalacetic transaminase in serum**, Clin. Chim. Acta, 7 (1962), pp. 199-205

[46] E. Amador, A.C. Salvatore**Serum glutamic oxalacetic transaminase activity: revised manual and automated methods using diazonnium dyes**, Am. J. Clin. Pathol., 55 (1971), pp. 686-697
[47] M.C. Scrutton, M.R. Olmsted, M.F. Utter**Pyruvate carboxylase from chicken liver**, Methods Enzymol., 13 (1969), pp. 235-249
[48] C.A. Friedrich, D.C. Morizot, M.J. Siciliano, R.E. Ferrell**The reduction of aromatic alpha-keto acids by cytoplasmic malate dehydrogenase and lactate dehydrogenase**, Biochem. Genet., 25 (1987), pp. 657-669
[49] A. Alt**Overview of critical parameters for the design and execution of a high-throughput screen for allosteric ligands**, Curr. Protoc. Pharmacol., 74 (2016), 9.20.21-29.20.23
[50] J. Yang, R.A. Copeland, Z. Lai**Defining balanced conditions for inhibitor screening assays that target bisubstrate enzymes**, J. Biomol. Screen, 14 (2009), pp. 111-120